Global Open Access Journal of Science

Open Access | Literature Review | Chemical Engineering
2(1), 2026 | PP - 17 - 27

Multidisciplinary Journal ISSN - 3070-6173

Literature Review

Chemical Engineering

Analysis and Control of the Acetic Anhydride Hydrolysis Reaction

Lakshmi N Sridhar*

Chemical Engineering Department, University of Puerto Rico Mayaguez, PR 00681, USA

Abstract

Bifurcation analysis and Multiobjective Nonlinear Model Predictive Control is performed on acetic anhydride hydrolysis reaction in a CSTR. The MATLAB program MATCONT was used to perform the bifurcation analysis. The MNLMPC calculations were performed using the optimization language PYOMO in conjunction with the state-of-the-art global optimization solvers IPOPT and BARON. The bifurcation analysis revealed the existence of Hopf bifurcation points and limit points. The MNLMC converged on the Utopian solution. Hopf bifurcation points, which cause unwanted limit cycles, are eliminated using an activation function based on the tanh function. The limit points (which cause multiple steady-state solutions from a singular point) are very beneficial because they enable the Multiobjective Nonlinear Model Predictive Control calculations to converge to the Utopia point (the best possible solution) in the model.

Keywords: Bifurcation, Optimization, Control, Acetic-anhydride, CSTR

Background

CH_3COOH, acetic acid, is a simple organic acid known as one of the most prominent carboxylic acids in use in industries as well as in everyday applications. It is most famously known as the active ingredient in vinegar, in concentrations of 4-8% acetic acid in most commercial products, most notable in apple cider vinegar, which has become prominent in medical applications in relation to diets and nutrition, wellness programs, as well as in other industries such as chemical formulation, agriculture, among others. The primary use of acetic acid is within the food sector. As vinegar, acetic acid acts as a preservative, condiment, and antimicrobial agent. The acidity of acetic acid prevents the growth of harmful microorganisms; thus, it is used for preserving food through the process of pickling. Acetic acid is also known to enhance the properties of food substances by giving them a sour taste and thus enhancing their flavor. Moreover, it is also used as a food additive (E260) to preserve and increase the shelf life of food. Acetic acid is a significant chemical feedstock in industrial chemistry, used as a precursor in the production of many chemical compounds. Large quantities of acetic acid produced globally are used to produce vinyl acetate monomer, a vital chemical feedstock for polymers used in paints, adhesives, coatings, and textiles. Another major application of acetic acid includes the use of acetic anhydride, which is employed as a chemical feedstock in the preparation of cellulose acetate, used in making films for photography, fibers, and plastic. In addition, acetic acid acts as a solvent and chemical medium in chemical reactions owing to its polarity and capacity to dissolve both organic and inorganic compounds. Acetic acid has various medical and healthcare applications. It has traditionally been used as an antiseptic when applied topically due to its ability to prevent the growth of bacteria and yeast. The diluted acetic acid solution is often used to treat ear infections, wounds, and skin ailments. In diagnostic medicine, acetic acid is used when the visual inspection method is required, as in cervical cancer screening. The purpose of its application

Correspondence:
Lakshmi. N Sridhar, Chemical Engineering Department, University of Puerto Rico Mayaguez, PR 00681, USA, ORCID id: 0000-0002-1024-1778, Email: lakshmin.sridhar@upr.edu

Received Dates: April 03, 2026;
Accepted Date: April 22, 2026;
Published Date: April 25, 2026:

Cite this article as: Sridhar LN, Analysis and Control of the Acetic Anhydride Hydrolysis Reaction, Glob. Open Access J. Sci, 2026; 2(1):17-27.

is solely based on its property of providing contrast when distinguishing abnormal tissues. It is cheap and often used in settings where healthcare is limited. In agriculture, acetic acid is used as a biological herbicide and soil treatment. As a dehydrating agent for cells, acetic acid is effective in inhibiting weed growth at particular concentrations. Unlike other pesticides, acetic acid readily degrades in the natural environment, leading to no persistent effects. In silage preservation, the main role of acetic acid is to prevent unwanted bacterial growth during storage. Another application of acetic acid is in environmental and biotechnology uses. It is an important key compound in anaerobic digestion and fermentation cycles, where it acts as a substrate for methanogenic bacteria. In wastewater treatment plants, acetic acid is used as a supplementary carbon source for improving nutrient removal in biological processes such as denitrification. In conclusion, acetic acid is a versatile and very useful chemical compound. The effectiveness of acetic acid, whether used as a preservative, chemical intermediate, disinfectant, or biodegradation agent, translates into its impact on modern society. The application and research on acetic acid continue to be essential for improving industrial processes and community health. The hydrolysis of acetic anhydride usually produces acetic acid. The hydrolysis of acetic anhydride to acetic acid, CH_3COOH, is an exothermic reaction, in liquid phase, catalyzed by sulfuric acid. The hydrolysis of acetic anhydride to form acetic acid is an elementary chemical reaction that finds paramount significance in the lab and industry. Acetic anhydride, written $(CH_3CO)_2O$, is an unstable and highly reactive chemical anhydride and is mostly utilized as an acetylating reagent, but on exposure to water, it hydrolyzes to form acetic acid, the major product of the hydrolysis reaction, which is an apt demonstration of nucleophilic acyl substitution and provides insight into the principles of reaction kinetics and thermodynamics, apart from chemical safety.

Acetic acid finds widespread application in the pharmaceutical sector owing to its versatility, availability, and well-understood safety profile. It serves as an important active ingredient and intermediate in the synthesis of several active pharmaceutical ingredients and excipients. Acetic acid and its derivatives are used in the production of acetylated compounds, which are employed to enhance the stability, bioavailability, and effectiveness of pharmaceutical compounds. One such widely known application of acetic acid is found in the production of acetylsalicylic acid, or aspirin, where the derivatives of acetic acid play an integral part in the formation of the acetyl group responsible for the analgesic actions of the compound.

Industrially, the hydrolysis of acetic anhydride is important in the controlled synthesis of acetic acid and in the treatment of wastes that contain traces of acetic anhydride, which then need to be neutralized. Acetic acid, on the other hand, is a desirable product that can be applied in various applications, including the synthesis of polymers, solvents, pharmaceuticals, and food additives. Its hydrolysis reaction, therefore, assumes importance in the precise synthesis of the product. Overall, the hydrolysis of acetic anhydride to form acetic acid is a straightforward chemical process from a laboratory perspective but complex at the conceptual level. The reaction (that is usually carried out in a CSTR) is

Acetic Anhydride $(CH_3CO)_2$ O+ water(H_2O) = Acetic Acid($2CH_3COOH$).

Acetic anhydride hydrolysis to acetic acid is a classic example of a chemically nonlinear reaction system. One source of nonlinearity arises from the reaction kinetics since the hydrolysis rate depends nonlinearly on both reagent concentrations; in many practical situations, water is in large excess, and pseudo-first-order approximations may hold. However, when water is not in overwhelming excess, the rate law is genuinely nonlinear, taking the multiplicative form with respect to the concentration variables. In addition, the reaction is autocatalytic: the product, acetic acid, can act as an acid by protonation, increasing the proton concentration and hence accelerating hydrolysis. This feedback between the product formation and the reaction rate introduces strong nonlinearity and may result in time-dependent acceleration of the reaction rate. Thermal effects even further reinforce the nonlinear behavior. The hydrolysis of acetic anhydride is exothermic-that is, heat is released and tends to increase the system temperature. Since reaction rates usually exhibit Arrhenius-type temperature dependence, even modest increases in temperature can substantially increase the reaction rate. This coupling between reaction progress and temperature creates a nonlinear interaction between the mass and energy balances, particularly in poorly mixed or adiabatic systems.

The hydrolysis of acetic anhydride proceeds rapidly and exothermically and also catalyzes autocatalytic reactions, raising serious concerns about its applications in industrial pharmacy and chemical production. This process of hydrolysis generates acetic acid when it comes into contact with water. This makes properly controlling moisture levels crucial for maintaining the stability of pharmaceuticals.

Additionally, nonlinearities result from transport and mixing effects. In heterogeneous or partially mixed systems, either water or acetic anhydride may develop local concentration gradients, leading to spatially nonuniform reaction rates. Complex transient behavior can result from the mutual interaction of diffusion, convection, and nonlinear reaction kinetics. The hydrolysis of acetic anhydride illustrates how feedback mechanisms, temperature dependence, and coupled mass–energy interactions produce nonlinear dynamics, even in chemically simple reactions.

Literature Review

Gray & Roberts, (1988) analysed chemical kinetics systems over the entire parameter space, investigating Isothermal oscillators Haldar & Rao,(1991) performed experimental studies on the limit cycle behavior of the sulphuric acid-catalyzed hydrolysis of acetic anhydride in a CSTR. Asprey (et al. 1996) studied the application of temperature scanning in kinetic investigations of the hydrolysis of acetic anhydride. Elnashaie & Elshishini, (1996) studied the Chaotic Behaviour of Gas-Solid Catalytic Reactors. Hirota (et al. 2010) studied the non-adiabatic calorimetric determination of kinetics and heat exchange for the hydrolysis of acetic anhydride. Jayakumar (et al. 2011) conducted an experimental and theoretical investigation

of the parameter sensitivity and dynamics of a continuous stirred-tank reactor for the acid-catalyzed hydrolysis of acetic anhydride. Asiedu (et al. 2013) developed a kinetic model of the hydrolysis of acetic anhydride at high temperatures using a diabatic batch reactor. Ball (2013) demonstrated the existence of thermal oscillations in the decomposition of organic peroxides. Ojeda-Toro (et al. 2016) performed dynamic modeling studies and bifurcation analysis for the methyl isocyanate hydrolysis reaction. Gómez García (et al. 2016) studied the thermal stability of the acetic anhydride hydrolysis reaction.

In this work, bifurcation analysis and multiobjective nonlinear model predictive control are performed for an acetic anhydride hydrolysis reaction in a CSTR using the model described by Gómez García (et al. 2016). The main contribution of this paper is to demonstrate the existence of limit cycles in the anhydride hydrolysis reaction in a CSTR and the use of an activation factor to eliminate them. The paper is organized as follows. First, the model equations are presented, followed by a discussion of the numerical techniques involving bifurcation analysis and Multiobjective Nonlinear Model Predictive Control (MNLMPC). The results and discussion are then presented, followed by the conclusions.

Model Equations Gómez García (et al. 2016)

The original dynamic model Gómez García (et al. 2016) for the acetic anhydride hydrolysis production in a CSTR is given by the set of equations

$$V_R\frac{dC_A}{dt}=\nu(C_{A0}-C_A)-A_0C_S\exp(-E/RT)C_AV_R$$

$$(V_R\rho C_P+w_s)\frac{dT}{dt}=\nu\rho C_P(T_0-T)+(-\Delta H_{rxn})A_0C_S\exp(-E/RT)C_AV_R-Ua(T-T_C)$$

$$(V_c\rho_cC_{Pc})\frac{dT_c}{dt}=Ua(T-T_C)+(V_c\rho_cC_{Pc})(T_{oc}-T)_c$$

.....(1)

T is the reaction temperature(K), and C_s and C_A are the sulfuric acid and acetic anhydride concentrations. T_c is the coolant temperature. The subscripts 0 and c indicate feed and cooling conditions, respectively. V_R is the reactor volume(m^3), ν represents the volumetric flow in (m^3/sec), A_0 represents the pre-exponential factor in (m^3/sec mol), E is the activation energy in J/mol and R is the gas constant. $\rho, C_p, w_s,$ represent the mixed reactive density(kg/m^3), the specific heat of reaction mixture(J/kg K), and the wall capacitance(J/K). Ua is the heat transfer coefficient (W/K) and ΔH_{rxn} is the reaction enthalpy (J/mol).

This model is scaled as follows.

$$x_a=\frac{C_A-C_{A0}}{C_{A0}};\gamma=\frac{E}{RT_0};\theta=(\frac{T-T_0}{T_0})\gamma;\theta_C=(\frac{T_C-T_0}{T_0})\gamma;\alpha=A_0C_S\exp(-\frac{E}{RT_0})t_r;\psi=\frac{-\Delta H_{rxn}C_{A0}V_R\gamma}{UAt_rT_0}$$

$$mpar=\frac{t_r}{t_{rc}};\tau=\frac{t}{t_r};dpar=\frac{Uat_r}{V_c\rho_cC_{pc}};\beta=\frac{-\Delta H_{rxn}C_{A0}V_R\gamma}{(\rho C_pV_R+w_s)T_0};bpar=\frac{\rho C_pV_R}{(\rho C_pV_R+w_s)}$$

The residence time is t_r. The variables $x_a;\gamma;\theta;\theta_C;\alpha;\psi;mpar;\tau;dpar;\beta;bpar$; represent the acetic anhydride conversion; the dimensionless activation energy; dimensionless temperature; dimensionless coolant temperature; the dimensionless rate constant; the Semenov number; residence time relation; dimensionless time; dimensionless cooling heat transfer; the dimensionless adiabatic temperature rise; and the capacitance relation. The scaled model equations are

$$\frac{d(x_a)}{d\tau}=-x_a+\left(\alpha e^{(\theta/(1+(\theta/\gamma)))}(1-x_a)\right)$$

$$\frac{d(\theta)}{d\tau}=(-bpar(\theta))+\left(\beta(1-x_a)\alpha e^{(\theta/(1+(\theta/\gamma)))}\right)-\left(\left(\frac{\beta}{\psi}\right)(\theta-\theta_c)\right) \quad (2)$$

$$\frac{d(\theta_c)}{d\tau}=dpar*(\theta-\theta_c)+(mpar*(\theta_{c0}-\theta_c))$$

The base parameters are

$$\alpha=0.25;\ \beta=28.226604;\ \gamma=35.9058;\ \psi=0.16392;$$

$$bpar=0.5079;\ dpar=1507.661;\ mpar=22.26258;\ \theta_{c0}=-2.35053.$$

More details about the model development are in Gómez García et al. (2016) [10]

Bifurcation Analysis

Bifurcation calculations are performed using the MATLAB software MATCONT. Bifurcation analysis explains the main causes for multiple steady states and limit cycles. Branch points and limit points cause multiple steady-state solutions while limit cycles and oscillatory behavior are causd by Hopf bifurcation points. The MATLAB program that effectively locates limit points, branch points, and Hopf bifurcation points is MATCONT. This program was developed and improved by several researhers (Dhooge Govearts, & Kuznetsov, 2003), (Dhooge Govearts, Kuznetsov, Mestrom & Riet, 2004). This program is very effective in identifying Limit Points (LP), Branch Points (BP), and Hopf bifurcation points (H) for a system of ordinary differential equations

$$\frac{dx}{dt}=f(x,\alpha) \quad .....(3)$$

$x\in R^n$ Where the bifurcation parameter is α. The gradient vesctor is orthogonal to the tangent and hence the tangent plane at any point $W=[w_1,w_2,w_3,w_4,....w_{n+1}]$ must satisfy

$$Aw=0 \quad .....(4)$$

The matrix *A* is defined by,

$$A=[\partial f/\partial x \quad |\partial f/\partial\alpha] \quad ....(5)$$

The sub-matrix $\partial f/\partial x$ is the Jacobian matrix. For both limit and branch points, the Jacobian matrix $J=(\partial f/\partial x)$ must have a determinant of 0.

At a limit point, there must exist only one tangent at the point of singularity. At this singular point, there is a one and only one non-zero vector, y, where *Jy=0.* This vector is of dimension n. Since there is only one tangent, the vector $y=(y_1,y_2,y_3,y_4,...y_n)$ must have the same direction with $\hat{w}=(w_1,w_2,w_3,w_4,...w_n)$. Since

$$J\hat{w}=Aw=0 \quad ..... (6)$$

the *n+1* th component of the tangent vector $w_{n+1} = 0$. This is the necessary condition for the existence of a a Limit Point (LP).

For a branch point, two tangents must exist at the point of singularity. Let the two tangents be z and w. This implies that

$$Az = 0$$
$$Aw = 0 \quad \text{.....(7)}$$

Imagine a vector v that is orthogonal to one of the tangent w. v can be expressed as a linear combination of *z* and *w* ($v = \gamma z + \delta w$). Since, $Az = Aw = 0$; $Av = 0$ and since w and v are orthogonal,

$w^T v = 0$. Hence, $Bv = \begin{bmatrix} A \\ w^T \end{bmatrix} v = 0$ which implies that B is singular. This implies that the necessary condition for the existence of a branch point is that the matrix $B = \begin{bmatrix} A \\ w^T \end{bmatrix}$ must be singular and have a determinant of 0.

At a Hopf bifurcation point,

$$\det(2 f_x(x,\alpha) @ I_n) = 0 \quad \text{.....(8)}$$

@ indicates the bialternate product while I_n is the n-square identity matrix. Hopf bifurcations cause limit cycles and should be eliminated because limit cycles make optimization and control tasks very difficult. More details can be found in Kuznetsov (1998, 2009) and Govaerts (2000) respectively.

Hopf bifurcations lead to limit cycles, which can cause equipment damage and make control tasks more difficult. They also produce less desirable products. The tanh activation function (where a control value u is replaced by it) is used to eliminate spikes in the optimal control profiles. Several researchers have shown this (Dubey et al 2022; Kamalov et al, 2021; Szandała, 2020; Sridhar 2023). Sridhar (2024) explained, with multiple examples, how the same activation factor involving the tanh function also effectively removes the limit-cycle-causing Hopf bifurcation points.

Multiobjective Nonlinear Model Predictive Control (MNLMPC)

Flores Tlacuahuaz (et al. 2012) originally developed a rigorous Multiobjective Nonlinear Model Predictive Control (MNLMPC) strategy. This procedure is used for performing the MNLMPC calculations. used. In a problem for which the variables $\sum_{t_i=0}^{t_i=t_f} q_j(t_i); j = 1, 2..., n$ have to be optimized

simultaneously, and the dynamic model is given by

$$\frac{dx}{dt} = F(x,u) \quad \text{... (9)}$$

t_f being the final time value, and n the total number of objective variables and *u* the control parameter. The single objective optimal control problem is solved independently for each of the variables $\sum_{t_i=0}^{t_i=t_f} q_j(t_i)$ and produces the values q_j^* . Then, the multiobjective optimal control (MOOC) problem that will be solved is

$$\min(\sum_{j=1}^{n} (\sum_{t_i=0}^{t_f} q_j(t_i) - q_j^*))^2 \quad \text{.....(10)}$$
$$subject\ to\ \frac{dx}{dt} = F(x,u);$$

This will provide the values of *u* at different times. The first control value of *u* obtained is used, and the remaining values are discarded. This procedure repeats until the implemented value matches the initial one, or the Utopia point ($\sum_{t_i=0}^{t_f} q_j(t_i) = q_j^*; j = 1, 2..., n$) is reached.

Pyomo.dae (Hart et al, 2017) is used for these calculations. Here, the differential equations are converted to a Nonlinear Program (NLP) using the orthogonal collocation method. The NLP is solved using IPOPT (Wächter & Biegler, 2006) and confirmed as a global solution with BARON (Tawarmalani & N. V. Sahinidis, 2005).

1. Sridhar (2024) demonstrated that when bifurcation analysis detects the presence of limit and branch points, the MNLMPC calculations converge to the Utopia solution. In this work, the singularity condition caused by the presence of the limit or branch points was applied to the co-state equation (Upreti, 2013). It was shown that the Lagrangian multipliers would be zero, rendering the constrained problem unconstrained, and the obtained optimal solution is the Utopia solution. Details can be found in Sridhar (2024)

Results and Discussion

Bifurcation Results

$\alpha; \psi; mpar; \theta_{c0}; bpar$ were used as the bifurcation parameters.

When bifurcation analysis is performed with α , as the bifurcation parameter (*bpar = 1.5079*), a limit point and a Hopf bifurcation point were found at $(x_a; \theta; \theta_c, \alpha)$ values of (0.774461, 4.001869, 3.909433, 0.093772) and (0.93221, 5.117611, 5.008938, 0.155975) (Figure 1a) . The limit cycle produced by this Hopf bifurcation point is shown in Figure 1b. When α is modified to $\frac{\alpha \tanh(\alpha)}{40}$ the Hopf bifurcation disappears (Figure 1c). The Hopf bifurcation causes an unwanted limit cycle which is eliminated using the activation factor.

When bifurcation analysis is performed with ψ , as the bifurcation parameter, a Hopf bifurcation point was found at $(x_a; \theta; \theta_c, \psi)$ Values of (0.931953, 4.505752, 4.405983, 0.117085). The limit cycle produced by this Hopf bifurcation point is shown in Figure 2b. When ψ is modified to $\frac{\psi \tanh(\psi)}{50}$ the Hopf bifurcation disappears (Figure 2c). The Hopf bifurcation causes an unwanted limit cycle which is eliminated using the activation factor.

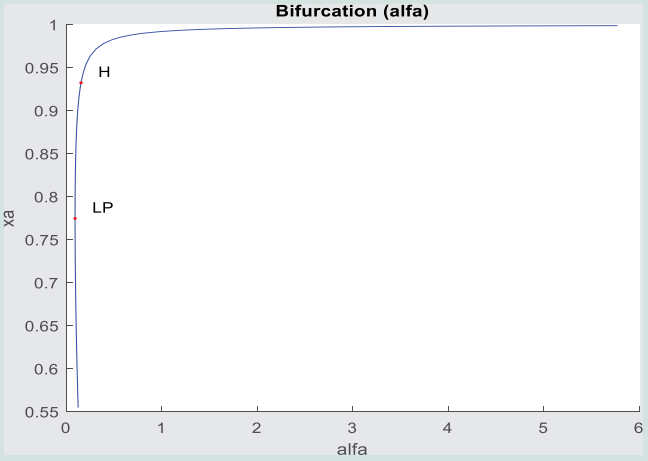

Figure 1a: Bifurcation Diagram with α as bifurcation parameter LP is the limit point; H is the Hopf bifurcation point.

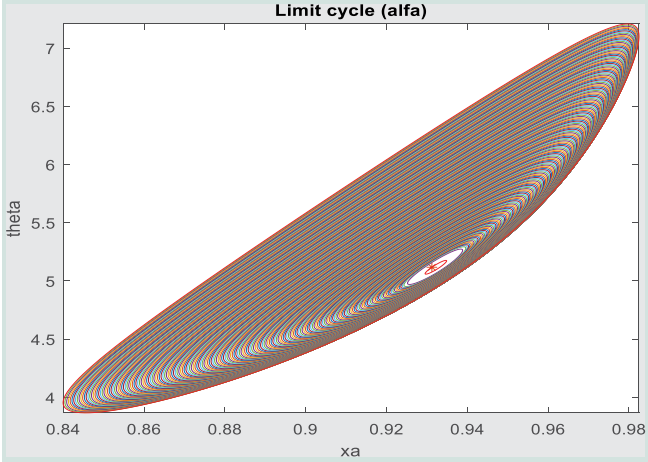

Figure 1b: Limit Cycle with as bifurcation parameter The limit cycle is shown in the theta xa surface.

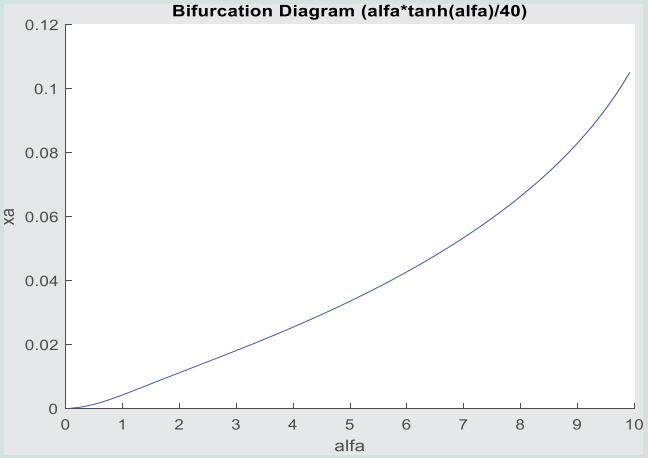

Figure 1c: Hopf bifurcation disappears when α is modified to $\frac{\alpha \tanh(\alpha)}{40}$ Both the Hopf bifurcation point and the limit points disappear when the activation factor is used.

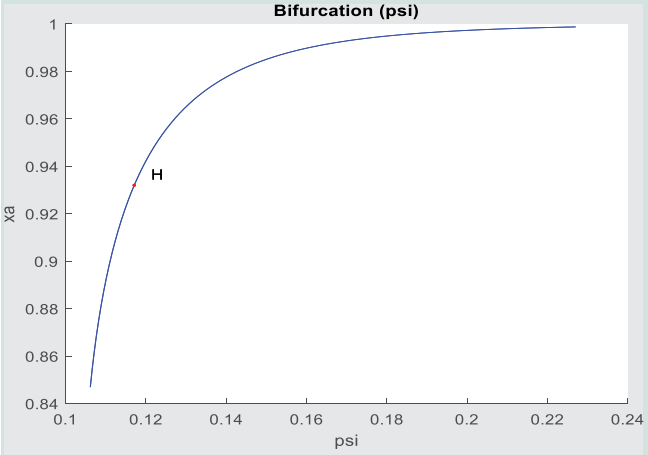

Figure 2a: Bifurcation Diagram with α as bifurcation parameter H is the Hopf bifurcation point

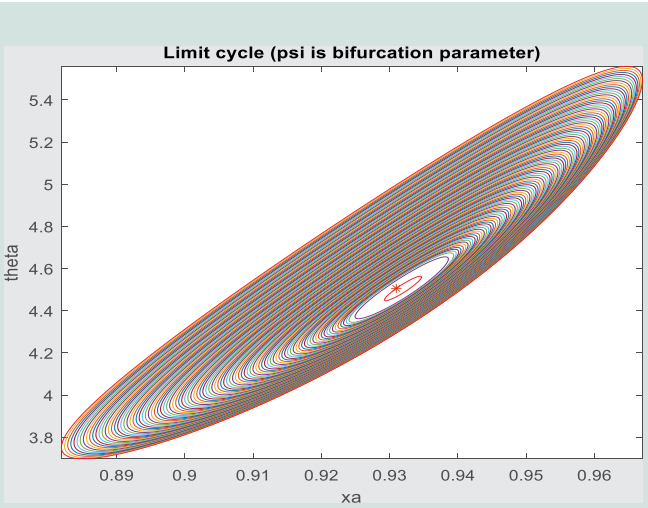

Figure 2b: Limit Cycle with α as bifurcation parameter. The limit cycle is shown in the theta xa surface

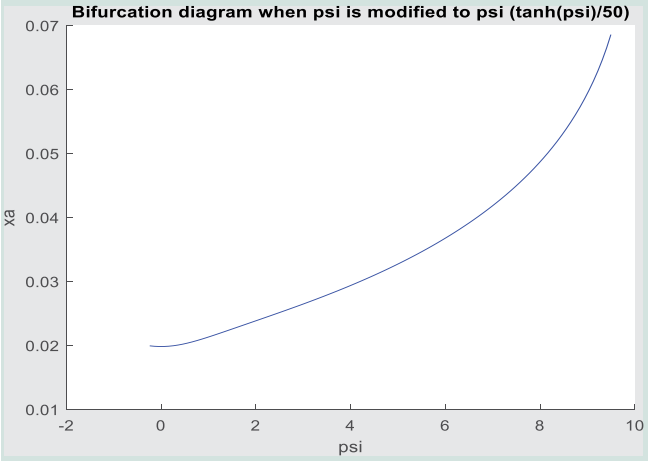

Figure 2c: Hopf bifurcation disappears when α is modified to $\frac{\psi \tanh(\psi)}{50}$ The activation factor eliminates the Hopf bifurcation.

When bifurcation analysis is performed with $mpar$, as the bifurcation parameter, a Hopf bifurcation point and two limit points were found at $(x_a;\theta;\theta_c,mpar)$ Values of (0.294831, 0.52173, 0.486853, 18.532201); (0.417464, 1.084921, 1.044463, 17.967077); and (0.523032, 1.54198, 1.496, 18.021763) (Figure 3a). The limit cycle produced by this Hopf bifurcation point is shown in Figure 3b.

When $mpar$ is modified to $\frac{mpar\tanh(mpar)}{0.008}$

the Hopf bifurcation disappears. (Figure 3c). The Hopf bifurcation causes an unwanted limit cycle which is eliminated using the activation factor.

When bifurcation analysis is performed with θ_{c0}, as the bifurcation parameter, two Hopf bifurcation points were found at $(x_a;\theta;\theta_c,\theta_{c0})$ values of (0.312933 0.610041 0.574473 -1.834224), and (0.920470 4.293647 4.253464 1.532214) (Figure 4a). Figures 4b and 4c show the limit cycles caused by these two Hopf bifurcation points. Both Hopf bifurcation points disappear, when θ_{c0} is modified to $\theta_{c0}\tanh(\theta_{c0})/50$ (Figure 4d). The Hopf bifurcation causes an unwanted limit cycle which is eliminated using the activation factor.

When bifurcation analysis is performed with $bpar$, as the bifurcation parameter, a Limit point and a Hopf bifurcation point were found at $(x_a;\theta;\theta_c,bpar)$ Values of (0.633355 2.042907 1.978976 3.413907); and (0.932533 4.517389 4.417451 2.048354) (Figure 5a). The limit cycle caused by this Hopf Bifurcation point is shown in Figure 5b.

The Hopf bifurcation disappears when $bpar$ is modified to $\frac{bpar\tanh(bpar)}{30}$ (Figure 5c). The Hopf bifurcation causes an unwanted limit cycle which is eliminated using the activation factor.

The use of the activation factor involving the tanh function causes the Hopf bifurcations to disappear, thereby validating the analysis in Sridhar (2024).

In the Continuous Stirred Tank Reactor (CSTR)

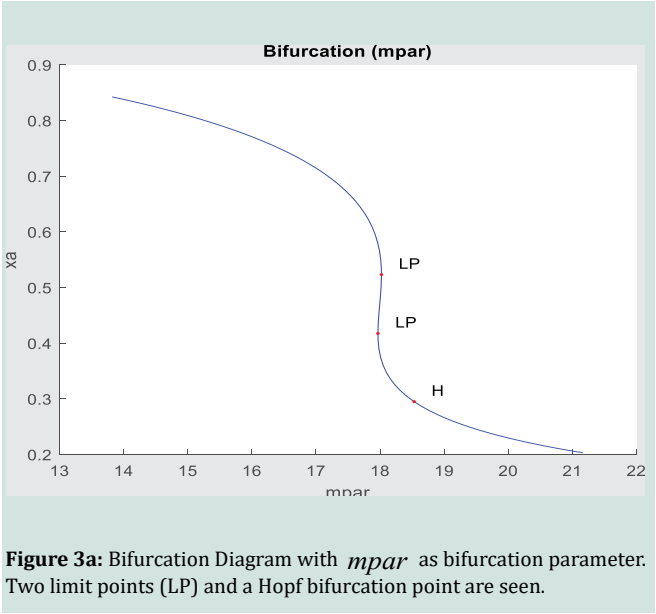

Figure 3a: Bifurcation Diagram with $mpar$ as bifurcation parameter. Two limit points (LP) and a Hopf bifurcation point are seen.

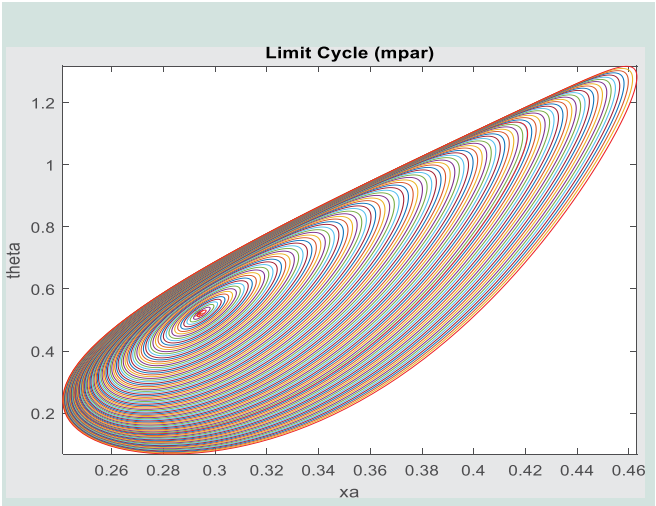

Figure 3b: Limit Cycle with $mpar$ as bifurcation parameter. The limit cycle is shown in the theta xa surface.

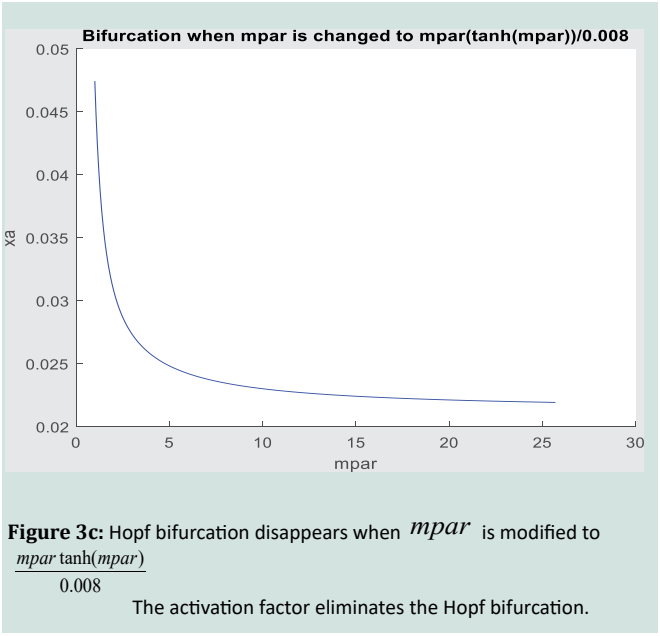

Figure 3c: Hopf bifurcation disappears when $mpar$ is modified to $\frac{mpar\tanh(mpar)}{0.008}$
The activation factor eliminates the Hopf bifurcation.

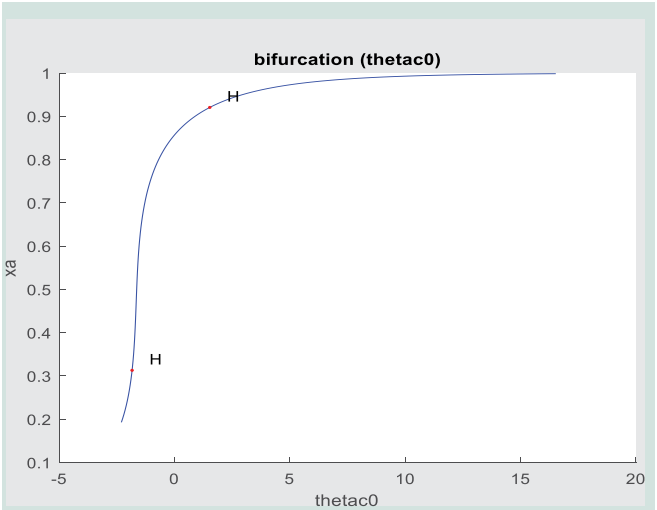

Figure 4a: Bifurcation Diagram with θ_{c0} as bifurcation parameter. Two Hopf bifurcation points (H) are seen.

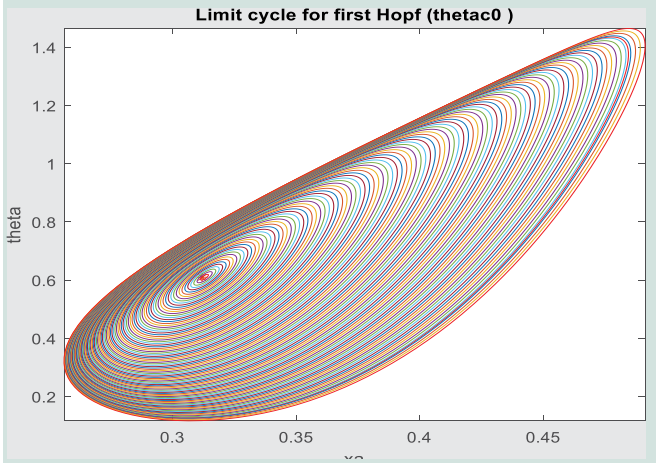

Figure 4b: Limit Cycle with first Hopf bifurcation point, with θ_{c0} as bifurcation parameter. The limit cycle is shown in the theta xa surface.

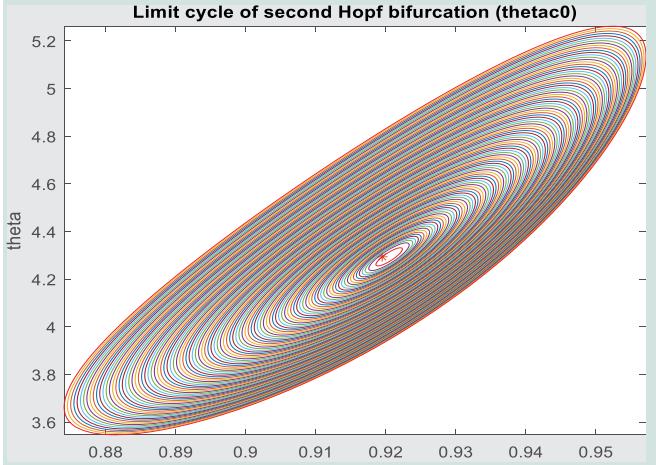

Figure 4c: Limit Cycle with second Hopf bifurcation point, with θ_{c0} as bifurcation parameter. The limit cycle is shown in the theta xa surface.

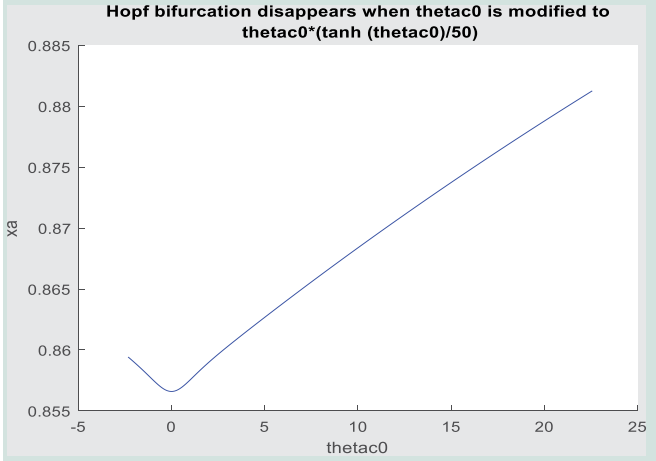

Figure 4d: Hopf bifurcation points disappear when θ_{c0} is modified to $\theta_{c0}\tanh(\theta_{c0})/50$.
The activation factor eliminates both the Hopf bifurcation points

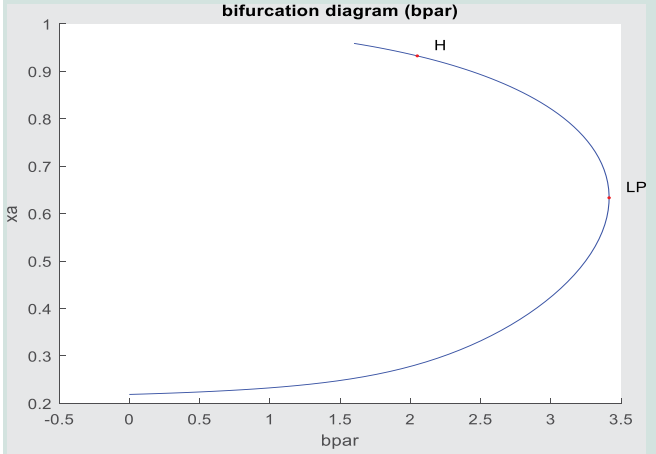

Figure 5a: Bifurcation Diagram with $bpar$ as bifurcation parameter. A Limit Point (LP) and a Hopf bifurcation point (H) are shown.

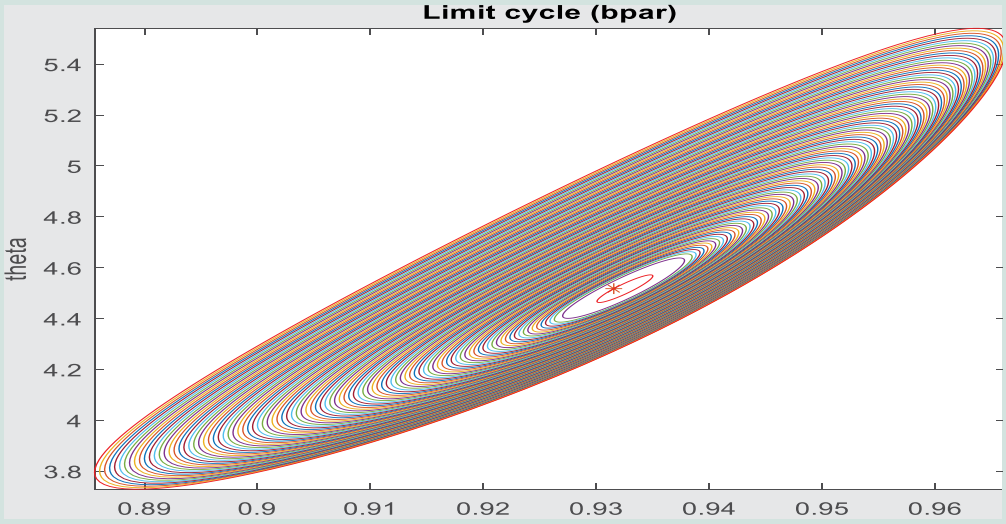

Figure 5b: Limit Cycle $bpar$ as bifurcation parameter. The limit cycle is shown in the theta xa plane.

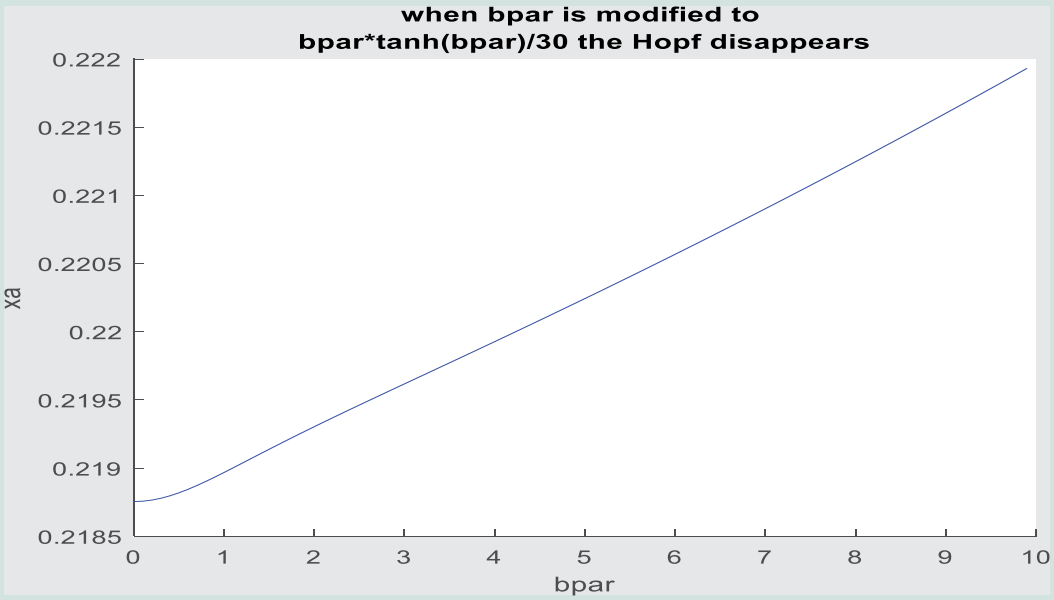

Figure 5c: Hopf bifurcation disappears when $bpar$ is modified to $\frac{bpar\tanh(bpar)}{30}$ The activation factor eliminates the Hopf bifurcation

undergoing acetic anhydride hydrolysis, the presence of limit cycles (caused by Hopf bifurcations) may significantly and negatively affect process performance, safety, and the quality of the reactor output. The hydrolysis of acetic anhydride is considered highly exothermic, and, together with the nonlinear dynamics of the continuous stirred tank reactor, this makes it possible for limit cycles to exist about oscillations in reactor states, such as temperature or concentration, without the influence of disturbances. One of the significant harmful effects of limit cycles is on temperature control. For example, in the CSTR reactor, temperature is known to affect reaction rates directly via Arrhenius kinetics. However, in limit cycles, the reactor temperature oscillates between higher and lower levels, rather than maintaining a constant level at its equilibrium state. If this is the case for the hydrolysis of Acetic Anhydride, higher temperatures significantly increase the rates of hydrolysis. Additionally, temperatures tend to rise above the safety threshold, thereby placing additional stress on the cooling mechanism, which could easily cause hydrolytic temperatures to run away. Low temperatures will result in reduced hydrolysis efficiency.

Limit cycles lead to concentrations of reactants or products that fluctuate, making downstream processing more difficult. For hydrolysis reactions, a constant rate of conversion of acetic anhydride to acetic acid is required to ensure the specifications of the final product. Varying concentrations result in varying outlet-stream compositions, complicating separation, purification, or analysis. The downstream processing apparatus operates based on constant feed rates. Variations may reduce the efficiency of downstream processing. Another adverse effect caused by CSTR reactors is decreased net conversion and yield. Although elevated temperatures that occur briefly due to oscillations can temporarily accelerate the reaction rate, the net result of the entire reaction cycle is likely to be less effective than the steady-state reaction. The decreased temperature and concentration portions of the cycling reaction result in a lower reaction level. Additionally, unused acetic anhydride can exit the reactor. Temperature variation leads to expansion and contraction of reactor walls, agitators, and heat-transfer surfaces. Material fatigue may result from prolonged expansion and contraction, gasket failure, and frequent equipment maintenance. Control and cooling valves are subject to endless modifications, which shortens their life. Limit cycles make process control and safety even more challenging. Linear control systems, designed around a fixed point, can be ineffective for controlling nonlinear oscillations. More specifically, the application of strong control can even increase these oscillations. This can also become a serious issue with a reactive, exothermic process like acetic anhydride hydrolysis, where it is rather challenging to distinguish oscillations from the onset of a dangerous runaway process. To conclude, the presence of limit cycles in a CSTR reacting with the hydrolysis of acetic anhydride creates several adverse effects on the system related to temperature, efficiency of the reaction, quality of the product, the life of the materials being utilized in the reactions, or the materials being reacted.

Hence, it is very important to eliminate the Hopf bifurcations that lead to limit cycles. The results show that incorporating the tanh activation function is highly effective at eliminating Hopf bifurcations.

Multiobjective Nonlinear Model Predictive Control (MNLMPC)

For the MNLMPC, the procedure described is followed. ψ is chosen as the control parameter, and

$$\sum_{t_i=0}^{t_i=t_f} x_a(t_i), \sum_{t_i=0}^{t_i=t_f} \theta_c(t_i)$$

were maximized individually, and led to a values of 1.9602

and 9.8947 The overall optimal control problem will involve the minimization of

$$(\sum_{t_{i=0}}^{t_i=t_f} x_a(t_i) - 1.9642)^2 + (\sum_{t_{i=0}}^{t_i=t_f} \theta_c(t_i) - 9.8947)^2$$

Was minimized subject to the model's equations. This led to a value of zero (the Utopia point). The MNLMPC values of the control variable ψ is 0.5064. The limit points cause the MNLMPC calculations to converge to the Utopia solution, validating the analysis of Sridhar (2024) Figures 6a, 6b, 6c, and 6d show the various MNLMPC profiles.

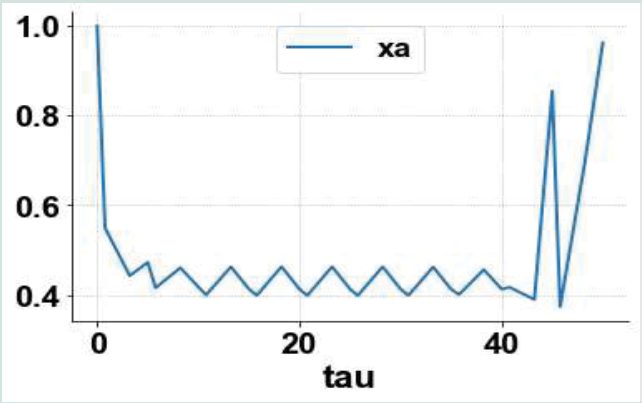

Figure 6a: MNLMPC $x_a - \tau$ xa-tau

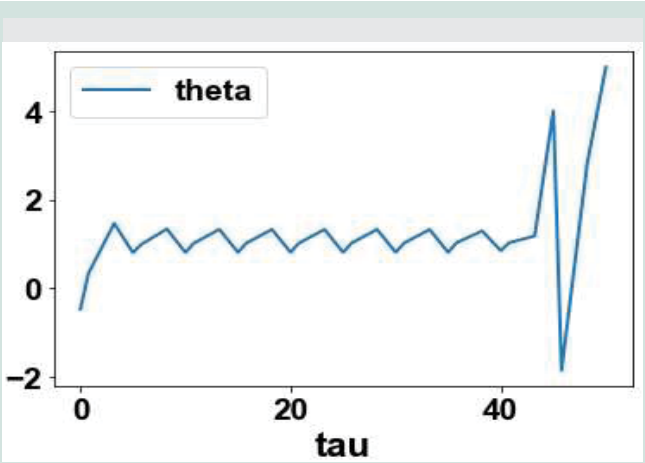

Figure 6b: MNLMPC $\theta - \tau$ theta –tau

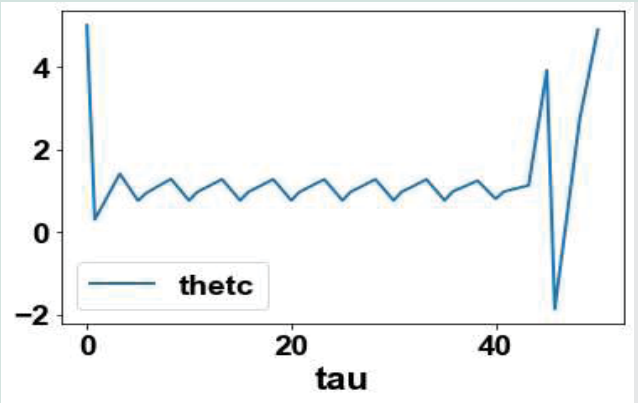

Figure 6c: MNLMPC $\theta_c - \tau$ thetc –tau

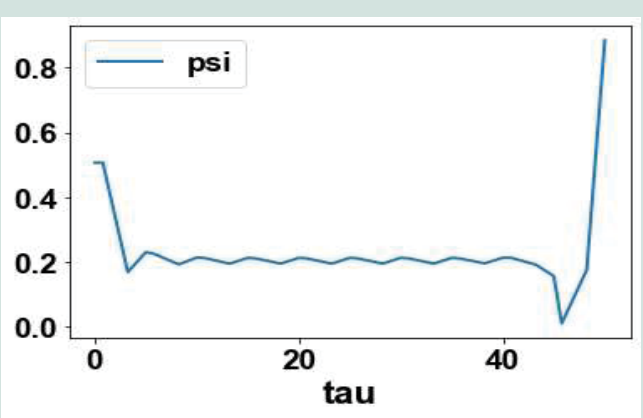

Figure 6d: MNLMPC $\psi - \tau$ psi -tau

Conclusions

Bifurcation analysis and multiobjective nonlinear control (MNLMPC) studies on acetic anhydride hydrolysis reaction in a CSTR . The bifurcation analysis revealed the existence of Hopf bifurcation points and limit points. Hopf bifurcation points, which cause unwanted limit cycles, are eliminated using an activation function based on the tanh function. The limit points (which cause multiple steady-state solutions from a singular point) are very beneficial because they enable the Multiobjective nonlinear model predictive control calculations to converge to the Utopia point (the best possible solution) in the models. A combination of bifurcation analysis and Multiobjective Nonlinear Model Predictive Control (MNLMPC) for the acetic anhydride hydrolysis reaction in a CSTR is the main contribution of this paper.

Acknowledgement

Dr. Sridhar thanks Dr. Carlos Ramirez for encouraging him to write single-author papers.

Data Availability Statement: All data used is presented in the paper.

All the data can be reproduced. All the code developed can be reproduced.

Conflicts of interest: No conflict of interest.

Funding: No funding received for this research.

.

References

- Gray, B.F., & Roberts, M.J. (1988). Analysis of chemical kinetics systems over the entire parameter space II: Isothermal oscillators. *Proceedings of the Royal Society of London A*, 416: 403-424. https://doi.org/10.1098/rspa.1988.0041
- Haldar, R., & Rao, D.P. (1991). Experimental studies on the limit cycle behavior of the sulphuric acid-catalyzed hydrolysis of acetic anhydride in a CSTR. *Chemical Engineering Science*, 46: 1197–1200. https://doi.org/10.1016/0009-2509(91)85115-E
- Asprey, S.P., Wojciechowski, B.W., Rice, N.M., & Dorcas, A. (1996). Applications of temperature scanning in kinetic investigations: The hydrolysis of acetic anhydride. *Chemical Engineering Science*, 51: 4681–4692. https://doi.org/10.1016/0009-2509(96)00306-5
- Elnashaie, S.S.E.H., & Elshishini, S.S. (1996). *Dynamic Modelling, Bifurcation and Chaotic Behaviour of Gas-Solid Catalytic Reactors*. Gordon and Breach Publishers, Amsterdam, The Netherlands.
- Hirota, W.H., Rodrigues, R.B., Sayer, C., & Giudici, R. (2010). Hydrolysis of acetic anhydride: Non-adiabatic calorimetric determination of kinetics and heat exchange. *Chemical Engineering Science*, 65: 3849–3858. https://doi.org/10.1016/j.ces.2010.03.028
- Jayakumar, N.S., Agrawal, A., Hashim, M.A., & Sahu, J.N. (2011). Experimental and theoretical investigation of parameter sensitivity and dynamics of a continuous stirred tank reactor for acid-catalyzed hydrolysis of acetic anhydride. *Computers & Chemical Engineering*, 35: 1295–1303. https://doi.org/10.1016/j.compchemeng.2010.09.005
- Asiedu, N., Hildebrandt, D., & Glasser, D. (2013). Kinetic modeling of the hydrolysis of acetic anhydride at high temperatures using a diabatic batch reactor (Thermos-Flask). *Journal of Chemical Engineering & Process Technology*, 4: 176. https://doi.org/10.4172/2157-7048.1000176
- Ball, R. (2013). Thermal oscillations in the decomposition of organic peroxides: Identification of a hazard, utilization, and suppression. *Industrial & Engineering Chemistry Research*, 52: 922–933. https://pubs.acs.org/doi/10.1021/ie301070d
- Ojeda-Toro, J.C., Dobrosz-Gómez, I., & Gómez-García, M.Á. (2016). Dynamic modeling and bifurcation analysis for the methyl isocyanate hydrolysis reaction. *Journal of Loss Prevention in the Process Industries*, 39: 106–111. https://doi.org/10.1016/j.jlp.2015.11.014
- Gómez García, M.Á., Dobrosz-Gómez, I., & Ojeda Toro, J.C. (2016). Thermal stability and dynamic analysis of the acetic anhydride hydrolysis reaction. *Chemical Engineering Science*, 142: 269–276. https://doi.org/10.1016/j.ces.2015.12.003
- Dhooge, A., Govaerts, W., & Kuznetsov, Y.A. (2003). MATCONT: A MATLAB package for numerical bifurcation analysis of ODEs. *ACM Transactions on Mathematical Software*, 29(2): 141–164. https://dl.acm.org/doi/10.1145/779359.779362
- Dhooge, A., Govaerts, W., Kuznetsov, Y.A., Mestrom, W., & Riet, A.M. (2004). CL_MATCONT: A continuation toolbox in MATLAB.161-166. https://doi.org/10.1145/952532.952567
- Kuznetsov, Y.A. (1998). *Elements of Applied Bifurcation Theory*. Springer, New York.
- Kuznetsov, Y.A. (2009). *Five Lectures on Numerical Bifurcation Analysis*. Utrecht University, Netherlands.
- Govaerts, W.J.F. (2000). *Numerical Methods for Bifurcations of Dynamical Equilibria*. SIAM.
- Dubey, S.R., Singh, S.K., & Chaudhuri, B.B. (2022). Activation functions in deep learning: A comprehensive survey and benchmark. *Neurocomputing*, 503: 92–108. https://doi.org/10.1016/j.neucom.2022.06.111
- Kamalov, A.F., Nazir, M., Safaraliev, A.K., Cherukuri, R., & Zgheib, R. (2021). Comparative analysis of activation functions in neural networks. *2021 28th IEEE International Conference on Electronics, Circuits, and Systems (ICECS)*, Dubai, United Arab Emirates: 1–6. https://doi.org/10.1109/ICECS53924.2021.9665646
- Szandała, T. (2020). Review and comparison of commonly used activation functions for deep neural networks. https://doi.org/10.1007/978-981-15-5495-7
- Sridhar, L.N. (2023). Bifurcation analysis and optimal control of the tumor macrophage interactions. *Biomedical Journal of Scientific & Technical Research*, 53(5): BJSTR.MS.ID.008470. https://doi.org/10.26717/BJSTR.2023.53.008470
- Sridhar, L.N. (2024). Elimination of oscillation causing Hopf bifurcations in engineering problems. *Journal of Applied Mathematics*, 2(4): 1826. https://doi.org/10.59400/jam1826
- Flores-Tlacuahuac, A., Morales, P., & Rivera Toledo, M. (2012). Multiobjective nonlinear model predictive control of a class of chemical reactors. *Industrial & Engineering Chemistry Research*: 5891–5899. https://pubs.acs.org/doi/10.1021/ie201742e
- Hart, W.E., Laird, C.D., Watson, J.-P., Woodruff, D.L., Hackebeil, G.A., Nicholson, B.L., & Siirola, J.D. (2017). *Pyomo – Optimization Modeling in Python* (2nd ed., Vol. 67).
- Wächter, A., & Biegler, L.T. (2006). On the implementation of an interior-point filter line-search algorithm for large-scale nonlinear programming. *Mathematical Programming*, 106: 25–57. https://doi.org/10.1007/s10107-004-0559-y
- Tawarmalani, M., & Sahinidis, N.V. (2005). A polyhedral branch-and-cut approach to global optimization. *Mathematical Programming*, 103(2): 225–249. https://link.springer.com/article/10.1007/s10107-005-0581-8

- Sridhar, L.N. (2024). Coupling bifurcation analysis and multiobjective nonlinear model predictive control. *Austin Chemical Engineering*, 10(3): 1107.
- Upreti, S.R. (2013). *Optimal Control for Chemical Engineers*. Taylor & Francis.

Cite this article as: Cite this article as: Sridhar LN, Analysis and Control of the Acetic Anhydride Hydrolysis Reaction, Glob. Open Access J. Sci, 2026; 2(1):17-27.